

Supporting Information

High-Yield Production of Few-Layer Boron Nanosheets for Efficient Electrocatalytic N₂ Reduction

Qun Fan,^a Changhyeok Choi,^b Chao Yan,^c Yongchao Liu,^c Jieshan Qiu,^a Song Hong,^{*d}
Yousung Jung ^{*b} and Zhenyu Sun ^{*a}

Experimental

Materials

All chemicals used in this work were of analytical grade and used without further treatments. Bulk boron, *N,N*-dimethylformamide, dimethyl sulfoxide, *N*-methyl pyrrolidone, 1,3-dimethyl-2-imidazolidinone, cyclohexane, propylene carbonate, cyclohexanone, tetrahydrofuran, *N*-cyclohexyl-2-pyrrolidone, benzaldehyde, benzyl benzoate, γ -butyrolactone, chlorobenzene, cyclopentanone, dibenzyl ether, 1-octyl-2-pyrrolidone, 1-vinyl-2-pyrrolidone, *N*-methylformamide, 1-cyclohexyl-2-pyrrolidone, para-(dimethylamino) benzaldehyde, NaOH, and C₅FeN₆Na₂O were purchased from Aladdin. Ethanol, isopropanol, HCl (37%) were provided by Beijing Chemical Works. *N,N*-Dimethylpropyleneurea was purchased from Energy Chemical. NaClO was purchased from Macklin. Nafion membranes were provided by Alfa Aesar.

Exfoliation of boron

For different solvent comparison, 10 mg boron and 10 mL different solvents added into glass vial and sonicated 6 hr used bath ultrasonication (KQ5200DE, 400 W across four horns operating at 40 kHz frequency and 100% power). The bath was modified by the addition of a cooling water to control the bath temperature about 25 °C during sonication. Then the muddy liquid was centrifuged at a rate of 3000 rpm for 30 min to remove the remaining bulk material. The top two-thirds of the supernatant were collected for ultraviolet-visible spectrophotometer (Persee TU-1950). For test of different initial concentration or centrifugal speed, we only alter the initial concentration to 0.5, 1, 3, 5, 10, 20, 30, 50 mg mL⁻¹ or centrifugal speed to 500, 1000, 3000, 5000, 7000 rpm and the other experimental conditions did not change. For

stability test, 80 mg boron and 80 mL benzyl benzoate dispersed in flask. Then flask was sonicated 6 hr, centrifuged at a rate of 3000 rpm for 30 min and the supernatant were collected to test 30 days. As for extinction coefficient, 400 mg boron and 400 mL benzyl benzoate dispersed in 500 mL flask follow by sonication 6 hr and then centrifugation at a rate of 3000 rpm for 30 min. 5 mL dispersion was took out and diluted by benzyl benzoate at ratio of 1:0, 1:1, 1:2, 1:3,1:4, and 1:5. The diluted liquid was determined by spectrophotometry. The rest liquid was suction filtrated. The filter liquor was collected and measured volume while the filter cake was washed by ethanol several times, dried and weighing. It is worth noting that the absorbance divided by cell length (A/l) at wavelength $\lambda = 400$ nm.

Characterization

X-ray powder diffraction (XRD) was performed with a D/MAX-RC diffractometer operated at 30 kV and 100 mA with Cu K α radiation. XPS experiments were carried out using Thermo Scientific ESCALAB 250Xi instrument. The instrument was equipped with an electron flood and scanning ion gun. All spectra were calibrated to the C 1s binding energy at 284.8 eV. Raman spectra of bulk boron and boron sheets samples deposited on SiO₂/Si substrates were collected with a Renishaw in Via Raman microscope with a He/Ne Laser excitation at 532 nm (2.33 eV). Scanning electron microscopy (SEM) was carried out using a field emission microscope (FEI Quanta 600 FEG) operated at 20 kV. Transmission electron microscope (TEM) was conducted using a JEOL ARM200 microscope with 200 kV accelerating voltage. TEM samples were prepared by depositing a droplet of suspension onto a Cu grid coated with a lacey carbon film.

Cathode preparation

Typically, about 10 mg catalyst was dispersed in 2 mL solution of isopropanol, deionized water and 5 wt% Nafion solution (100: 100: 1) by sonicating for 30 min to form a homogeneous ink. 200 μ L of the dispersion was then loaded onto a carbon paper electrode with an area of 1 x 1 cm² and dried under ambient conditions. For linear sweep

voltammograms in Ar- or N₂-saturated 0.1 M HCl solution, 6 mg catalyst was dispersed in the mixture of 600 μL ethanol, 600 μL deionized water and 600 μL Nafion solution (1 wt%). Then it sonicated for 30 min to form a homogeneous ink. 7.95 μL of the dispersion was then loaded onto glassy carbon electrode and dried under ambient conditions.

Electrochemical measurements

Controlled potential electrolysis of N₂ was tested in an H-cell system, which was separated by a Nafion 117 membrane. Before NRR tests, the Nafion membrane was pretreated by heating in 5% H₂O₂ aqueous solution and 0.5 M H₂SO₄ at 80 °C for 1 h, respectively. Then the Nafion membrane was immersed in deionized water under ambient conditions for 30min and wash with deionized water. Toray carbon fiber paper with a size of 1 cm × 1 cm was used as working electrode. Pt wire and Ag/AgCl electrodes were used as counter electrode and reference electrode, respectively. The potentials were controlled by an electrochemical working station (CHI 760E, Shanghai CH Instruments Co., China). All potentials in this study were measured against the Ag/AgCl reference electrode and converted to the RHE reference scale by

$$E \text{ (vs. RHE)} = E \text{ (vs. Ag/AgCl)} + 0.21 \text{ V} + 0.0591 \times \text{pH} \quad (\text{Eq. S1})$$

Electrocatalytic reduction of N₂ was conducted in N₂-saturated 0.1 M HCl solution at room temperature and atmospheric pressure. N₂ was purged into the HCl solution for at least 30 min to remove residual air in the reservoir, then controlled potential electrolysis was performed at each potential for 60 min.

Linear sweep voltammograms in Ar- or N₂ atmosphere were carried out in a three-electrode system using Ag/AgCl as reference electrode, Pt wire as counter electrode and glassy carbon as working electrode on a CHI 760E potentiostat (CHI 760E., Shanghai CH Instruments Co., China). Rotating disk electrode (RDE) experiments were run on an AFMSRCE RDE control system (Pine Inc., USA). The electrolyte is 0.1M HCl solution and Ar or N₂ purged at least 30 min.

Determination of ammonia

Concentration of produced ammonia was spectrophotometrically determined by the indophenol blue method.¹ In detail, 2 mL aliquot of the solution was removed from the electrochemical reaction vessel. Then, 2 mL of a 1 M NaOH solution containing 5 wt% salicylic acid and 5 wt% sodium citrate was added, followed by addition of 1 mL of 0.05 M NaClO and 0.2 mL of 1 wt% C₅FeN₆Na₂O (sodium nitroferricyanide) aqueous solution. After 2 h of incubation at room temperature, the absorption spectrum was measured using an ultraviolet-visible spectrophotometer. The formation of indophenol blue was determined based on the absorbance at a wavelength of 655 nm. The concentration-absorbance curves were calibrated using standard ammonia chloride solutions, as shown in Figure S10b, which contained the same concentrations of HCl as used in the electrolysis experiments.

Determination of hydrazine

The formation of hydrazine during electrolysis was examined by the method of Watt and Chrisp.² A mixture of para-(dimethylamino) benzaldehyde (5.99 g), HCl (37%, 30 mL), and ethanol (300 mL) was used as a color reagent. To do calibration, a series of reference solutions were firstly prepared by pipetting suitable volumes of hydrazine hydrate-nitrogen 0.1 M HCl solution in colorimetric tubes. Then, 5 mL of diluted HCl electrolyte (pH 1) was prepared. Subsequently, 5 mL of the above prepared color reagent was mixed and stirred for 10 min at room temperature. Finally, the absorbance of the resulting solution was measured at 455 nm, and the yields of hydrazine were estimated from a standard curve using 5 mL of residual electrolyte and 5 mL of color reagent.

Calculation of the faradaic efficiency (FE) and the yield rate

The FE was calculated from the charge consumed for NH₃ generation and the total charge passed through the electrode:

$$FE = (3F \times c_{\text{NH}_3} \times V)/Q \quad (\text{Eq.})$$

S2)

The yield rate of NH₃ can be estimated using the following equation:

$$\text{Yield rate} = (c_{\text{NH}_3} \times V)/(t \times m) \quad (\text{Eq. S3})$$

S3)

where F is the faraday constant (96 485 C mol⁻¹), c_{NH_3} is the measured NH₃ concentration, V is the volume of the electrolyte, Q is the total charge passed through the electrode, t is the electrolysis time (2 h), and m is the metal mass or the total mass of the catalyst. The reported NH₃ yield rate, FE, and corresponding error bars were obtained based on the measurements of at least two separately prepared samples under the same conditions.

Computational details

Structure relaxation and total electronic energy calculations were performed using spin-polarized density functional theory (DFT) methods implemented in the Vienna *ab initio* simulation package (VASP) with projector-augmented wave (PAW) pseudopotential.³⁻⁶ We used RPBE exchange functional coupled with dispersion correction (D3).⁷⁻¹⁰ A cut-off energy for plane wave basis set was set to 400 eV.

We used primitive cell of β -boron containing 105 boron atoms. The bulk boron and surface slab models were calculated with the 4 x 4 x 4 Monkhorst-Pack mesh and gamma point sampling, respectively.¹¹ All surface slab models include 4~6 layers of boron atoms. Only the top most two layers and adsorbates were allowed to relax, while other layers were fixed to their optimized bulk positions. All slab models include 18 Å of vacuum along c-axis. The gas molecules (H₂, N₂ and NH₃) were calculated in a 15 Å × 15 Å × 15 Å box.

The computational hydrogen electrode (CHE) model developed by Nørskov and co-workers was employed to estimate free energy change in electrochemical reduction reactions.¹² Water can stabilize reaction intermediates of NRR, however, it can affect the overpotential for NRR by ~0.1 eV.¹³ Due to this small effect of water in NRR, we did not include solvation effects in this study.

Table S1. The absorbance (A_{400}) and boron nanosheet dispersion concentration after 6 h of ultrasonication followed by CF at 3000 rpm for 30 min in 21 different organic solvents

Solvent	A_{400}	Concentration/mg mL⁻¹
Isopropyl alcohol	0.013	0.00306
<i>N,N</i> -Dimethylformamide	0.00633	0.00149
Dimethyl sulfoxide	0.006	0.00141
<i>N</i> -Methyl pyrrolidone	0.02	0.00471
Cyclohexane	0	0
1,3-Dimethyl-2-imidazolidinone	0.02167	0.0051
Ethanol	0.003	7.06323E-4
Propylene carbonate	0.027	0.00636
Cyclohexanone	0.01667	0.00392
Tetrahydrofuran	0.003	7.06323E-4
<i>N</i> -Cyclohexyl-2-pyrrolidone	0.0175	0.00412
Benzaldehyde	0.00267	6.27842E-4
Benzyl benzoate	0.0445	0.01048
γ -Butyrolactone	0.029	0.00683
Chlorobenzene	0.01333	0.00314
Cyclopentanone	0.006	0.00141
Dibenzyl ether	0.009	0.00212
1-Octyl-2-pyrrolidone	0.01133	0.00267
1-Vinyl-2pyrrolidone	0.01867	0.00439
<i>N,N</i> -Dimethylpropyleneurea	0.017	0.004
<i>N</i> -Methylformamide	0.02167	0.0051



Fig. S1 Schematic illustration of ultrasonication-assisted liquid-phase exfoliation of boron. The photograph shows a Tyndall effect of the boron nanosheet dispersion, an indication of a colloidal stable nature.

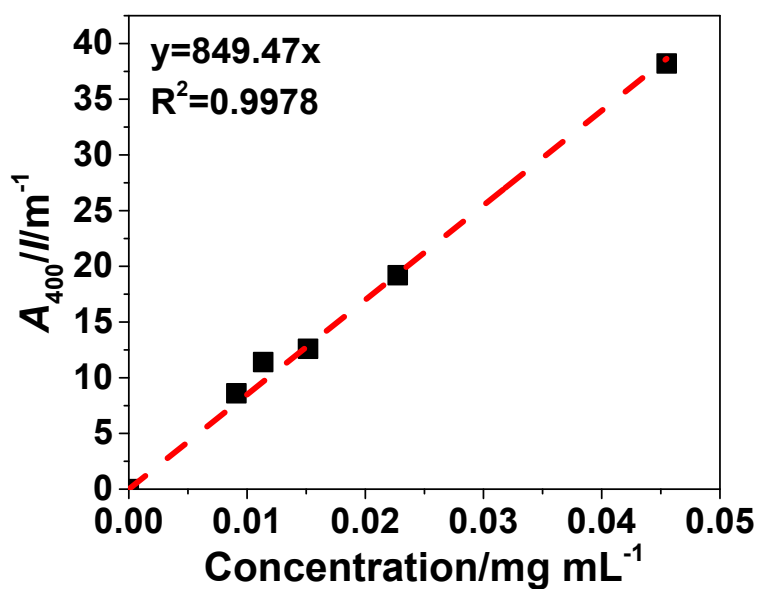


Fig. S2 Extinction coefficient of boron nanosheets.

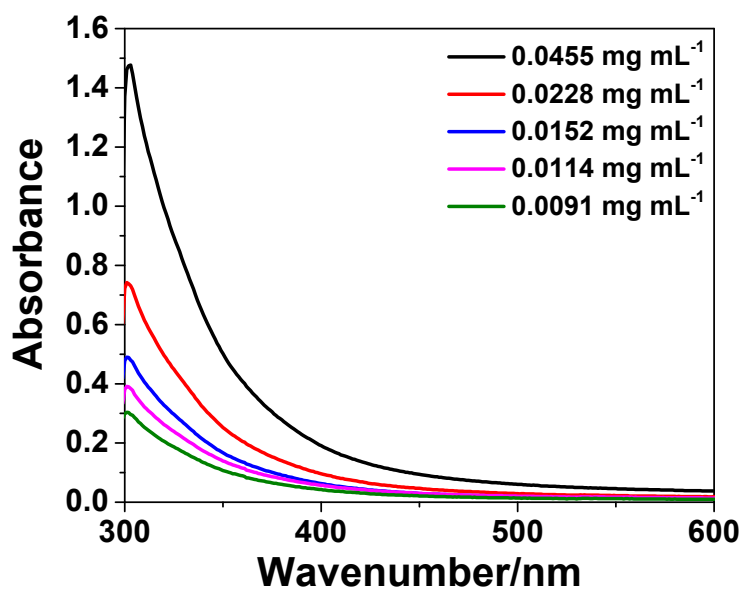


Fig. S3 Corresponding UV absorbance of Fig. S2.

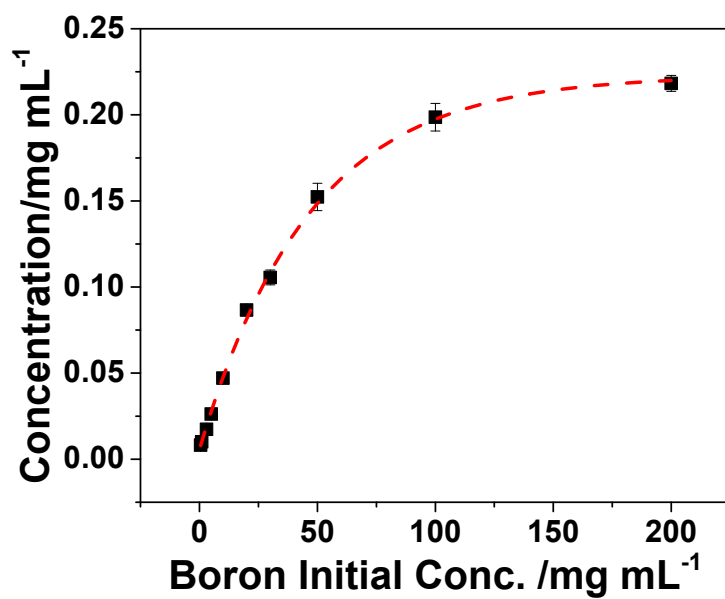


Fig. S4 Boron nanosheet dispersion concentration as a function of boron initial concentration.

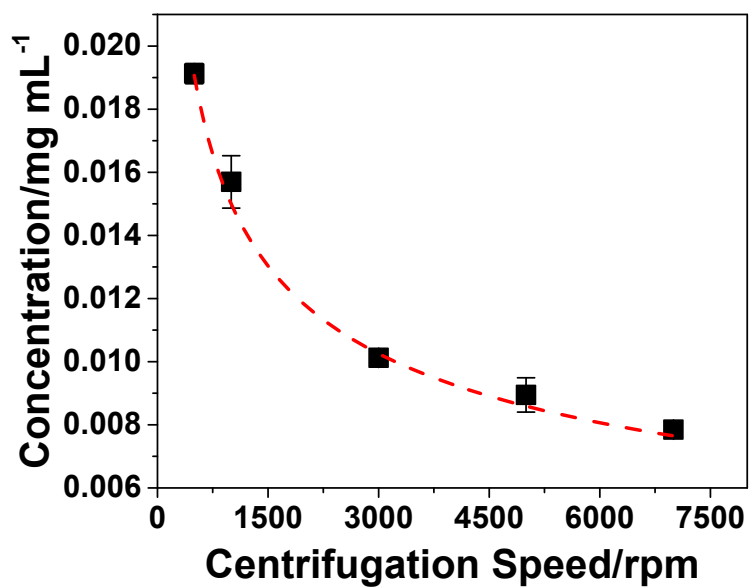


Fig. S5 Boron nanosheet dispersion concentration versus centrifugation speed.

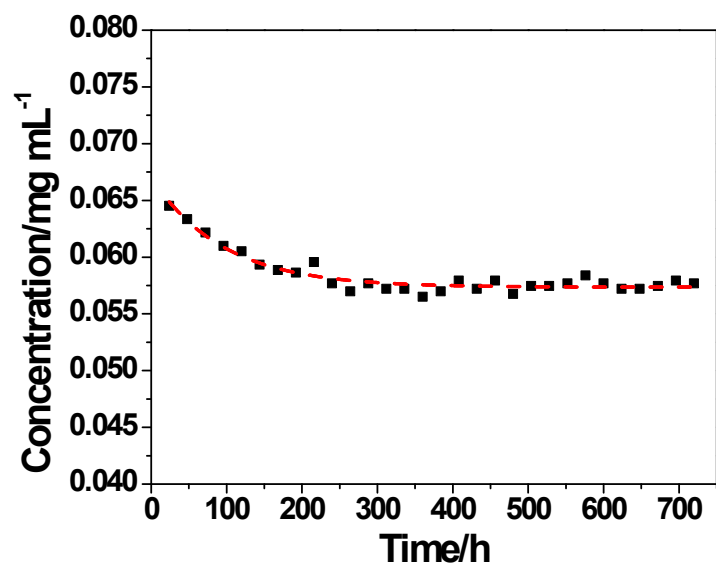


Fig. S6 Boron nanosheet dispersion concentration versus sedimentation time.

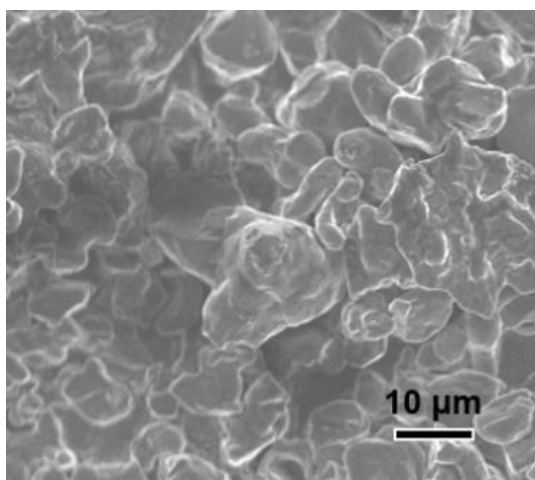


Fig. S7 SEM image of exfoliated boron nanosheets.

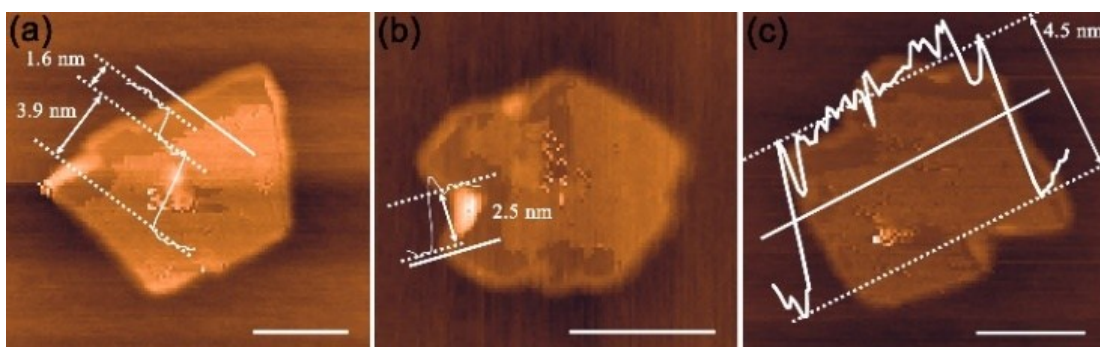
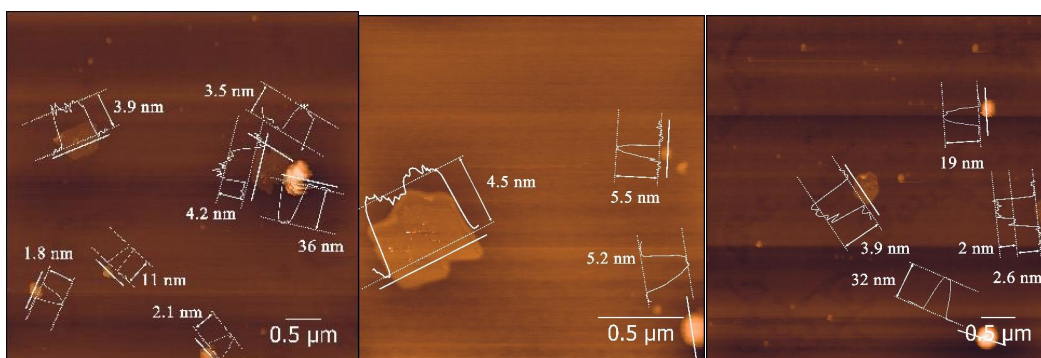


Fig. S8 (a)-(c) AFM images of the boron nanosheets with different thicknesses. The scale bars in all cases are 250 nm.



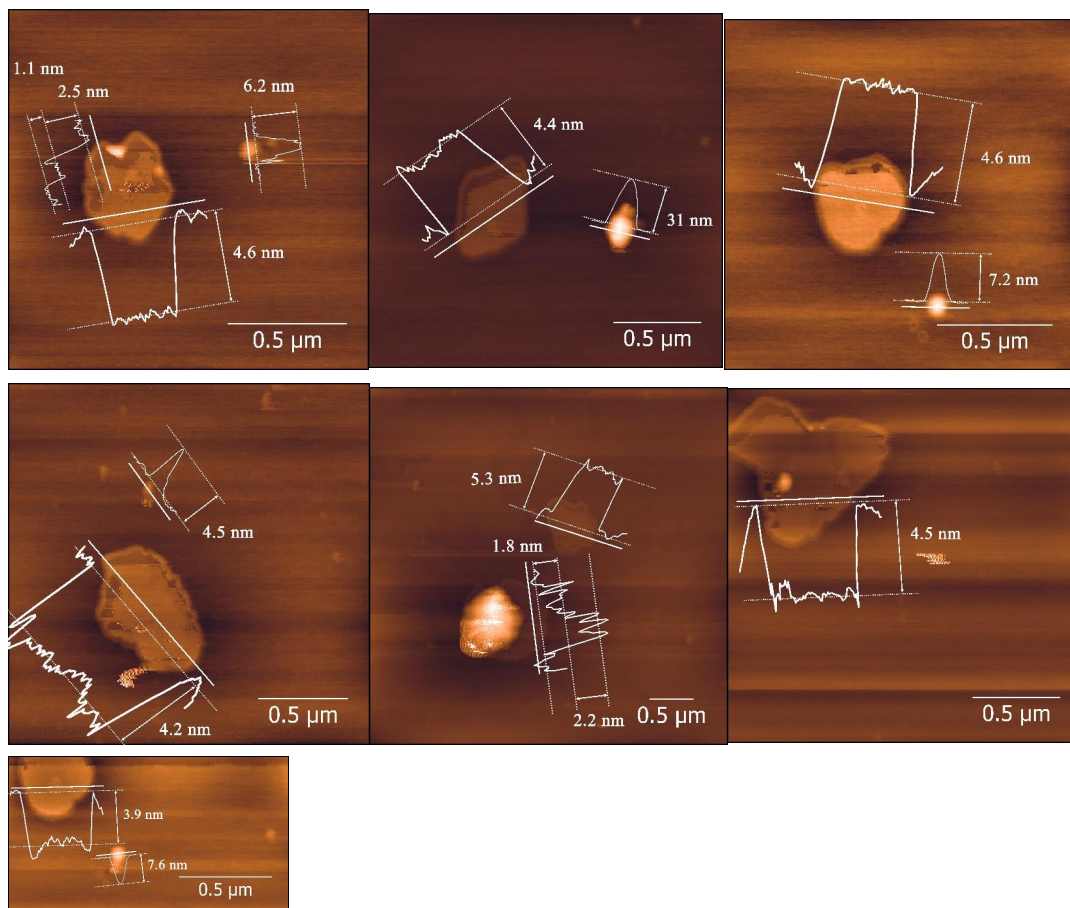


Fig. S9 AFM images of exfoliated boron nanosheets.

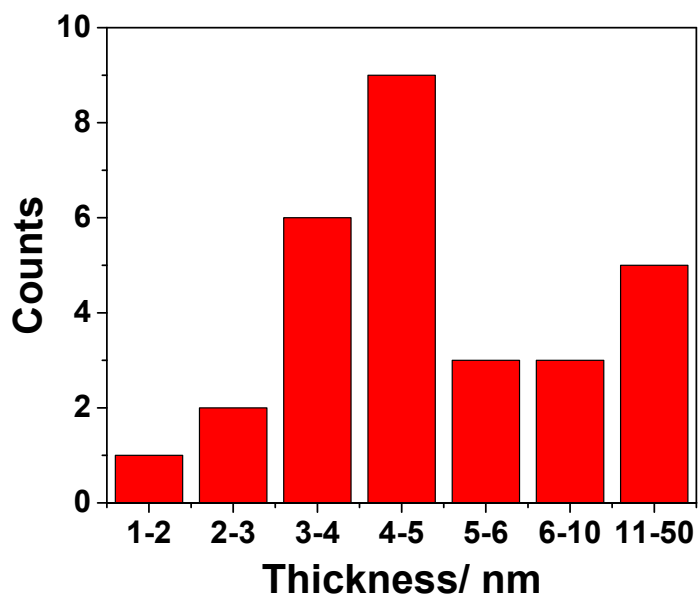


Fig. S10 Statistics of thickness of exfoliated boron nanosheets based on AFM estimation.

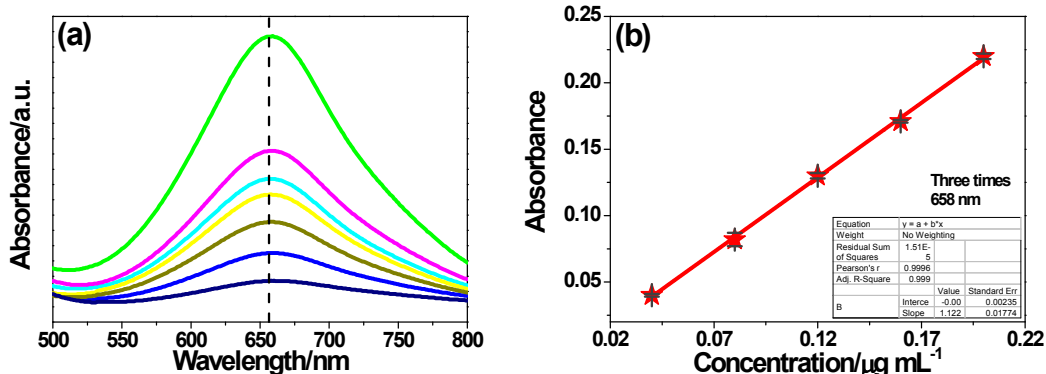


Fig. S11 (a) UV-vis curves of indophenol assays with NH_4^+ ions after incubated for 2 h at room temperature. (b) The calibration curve used for estimation of NH_3 by NH_4^+ ion.

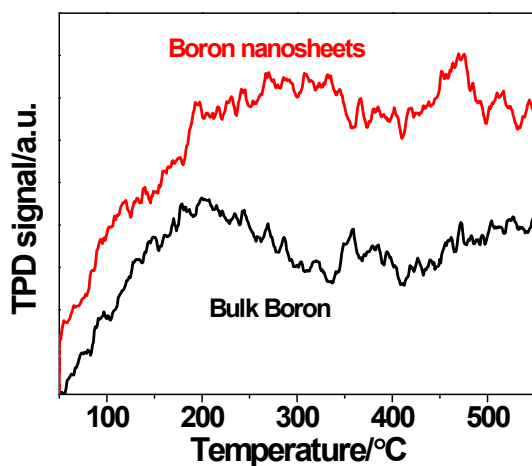


Fig. S12 N_2 TPD profiles of boron nanosheets and bulk boron.

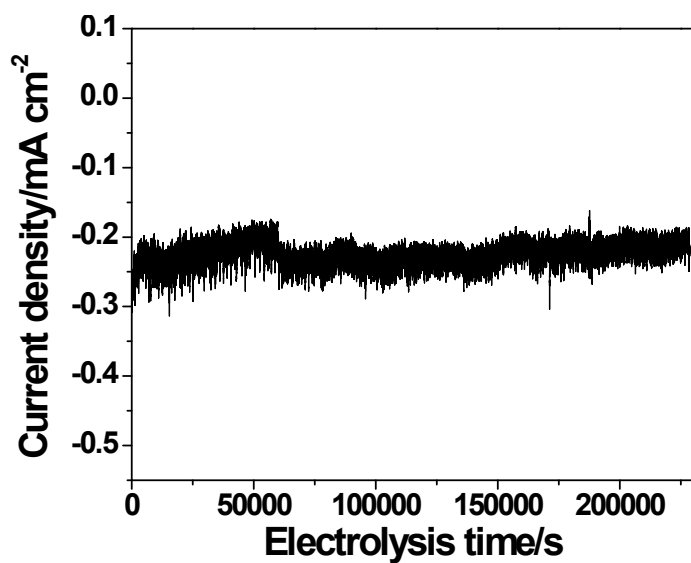


Fig. S13 Stability chronoamperometric curves.

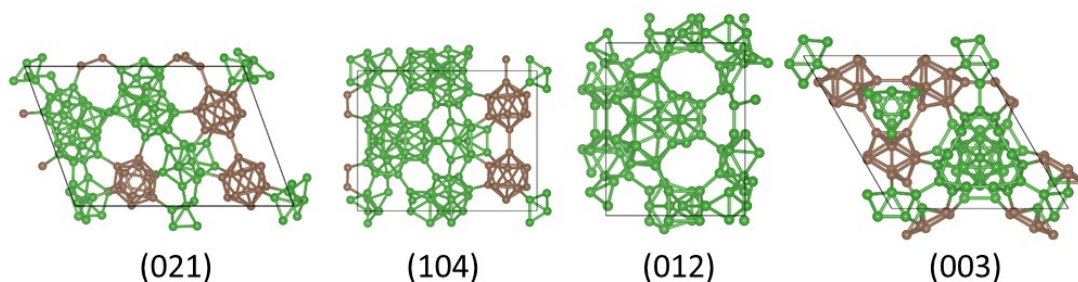


Fig. S14 Top-view of the optimized geometries of (021), (104), (012) and (003) surfaces of boron. Boron atoms in icosahedron are shown in brown, while other boron atoms are shown in green.

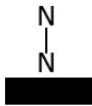
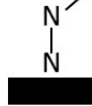
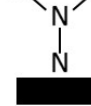
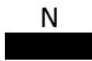

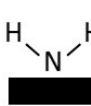
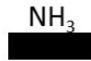
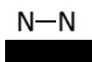
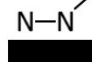
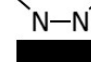
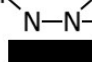
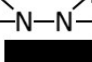
0	1	2	3	4	5	6
 $*N_2$	 $*NNH$	 $*NNH_2$	 $*N$	 $*NH$	 $*NH_2$	 $*NH_3$
 $*N_2$	 $*NNH$	 $*NHNH$	 $*NHNH_2$	 $*NH_2NH_2$		

Fig. S15 All possible reaction intermediates for NRR. Numbers in first row indicate the number of transferred proton and electron pairs ($H^+ + e^-$).

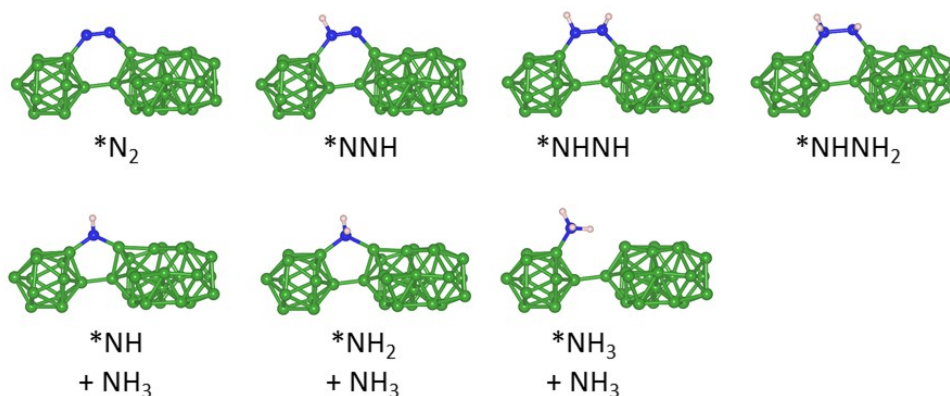


Fig. S16 Side-view of optimized geometries of reaction intermediates of ENR on (021)

surface of boron via the lowest energy requiring pathway. Green, blue and ivory balls represent boron, nitrogen and hydrogen atoms. The desorbed NH_3 is omitted for clarity.

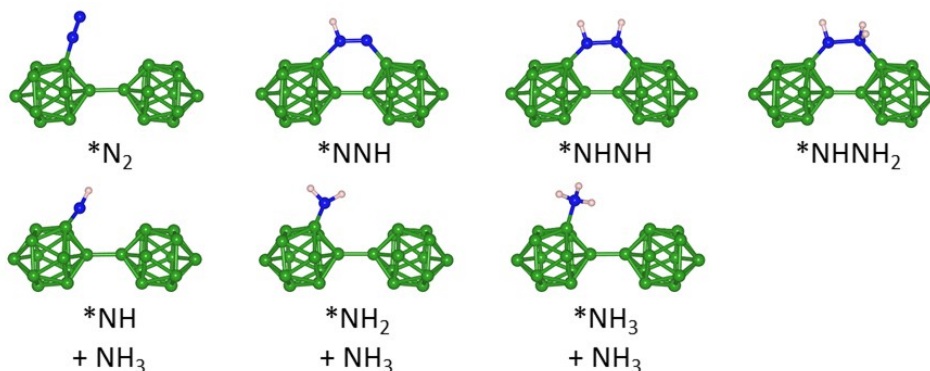


Fig. S17 Side-view of optimized geometries of reaction intermediates of ENR on (104) surface of boron via the lowest energy requiring pathway. Green, blue and ivory balls represent boron, nitrogen and hydrogen atoms. The desorbed NH_3 is omitted for clarity.

References

1. D. Zhu; L. H. Zhang; R. E. Ruther; R. J. Hamers, *Nature Materials*, 2013, **12**, 836-841.
2. G. W. Watt; J. D. Chrisp; A. Chem, *Analytical Chemistry*, 1963, **26**, 2006-2008.
3. P. E. Blöchl, *Physical Review B*, 1994, **50**, 17953-17979.
4. G. Kresse; J. Furthmüller, *Physical review B*, 1996, **54**, 11169.
5. G. Kresse; J. Furthmüller, *Computational Materials Science*, 1996, **6**, 15-50.
6. G. Kresse; D. Joubert, *Physical Review B*, 1999, **59**, 1758.
7. J. P. Perdew; K. Burke; M. Ernzerhof, *Physical review letters*, 1996, **77**, 3865.
8. B. Hammer; L. B. Hansen; J. K. Nørskov, *Physical Review B*, 1999, **59**, 7413.
9. S. Grimme; J. Antony; S. Ehrlich; H. Krieg, *The Journal of chemical physics*, 2010, **132**, 154104.
10. S. Grimme; S. Ehrlich; L. Goerigk, *Journal of computational chemistry*, 2011, **32**, 1456-1465.
11. H. J. Monkhorst; J. D. Pack, *Physical review B*, 1976, **13**, 5188.
12. J. K. Nørskov; J. Rossmeisl; A. Logadottir; L. Lindqvist; J. R. Kitchin; T. Bligaard; H. Jonsson, *The Journal of Physical Chemistry B*, 2004, **108**, 17886-17892.
13. J. H. Montoya; C. Tsai; A. Vojvodic; J. K. Nørskov, *ChemSusChem*, 2015, **8**, 2180-2186.